

## Vascular targeted radioimmunotherapy for the treatment of glioblastoma

<sup>1</sup>\*Katja Behling, <sup>2</sup>William F. Maguire, <sup>1</sup>José Carlos López Puebla, <sup>1</sup>Shanna R. Sprinkle,

<sup>1</sup>Alessandro Ruggiero, <sup>3</sup>Joseph O'Donoghue, <sup>4,5</sup>Philip H. Gutin, <sup>2,6</sup>David A. Scheinberg,

<sup>1,7</sup>\*\*Michael R. McDevitt

<sup>1</sup>Department of Radiology, Memorial Sloan Kettering Cancer Center, New York, New York;

<sup>2</sup>Department of Molecular Pharmacology, Memorial Sloan Kettering Cancer Center, New York, New York;

<sup>3</sup>Department of Medical Physics, Memorial Sloan Kettering Cancer Center, New

York, New York; <sup>4</sup>Department of Neurosurgery, Memorial Sloan Kettering Cancer Center, New

York, New York; <sup>5</sup>Department of Neurological Surgery, Weill Cornell Medical College, New

York, New York; <sup>6</sup>Department of Pharmacology, Weill Cornell Medical College, New York,

New York; <sup>7</sup>Department of Medicine, Weill Cornell Medical College, New York, New York

\*Katja Behling, Ph.D., Department of Radiology, Memorial Sloan Kettering Cancer Center, 1275 York Avenue, Box 231, New York, New York 10065, (646) 888-2205 Tel, (646) 422-0640 Fax, behlingk@mskcc.org.

\*\*Corresponding author: Michael R. McDevitt, Ph.D., Department of Radiology, Memorial Sloan Kettering Cancer Center, 1275 York Avenue, Box 231, New York, New York 10065, (646) 888-2192 Tel, (646) 422-0640 Fax, m-mcdevitt@ski.mskcc.org.

### Key Words:

Radioimmunotherapy (RIT)

Actinium-225 (<sup>225</sup>Ac)

Glioblastoma

Vascular endothelium (VE)

### Disclosure of Potential Conflicts of Interest

M. R. McDevitt and D. A. Scheinberg declare associations with Actinium Pharmaceuticals, Inc.

**Word count:** 5070

**Running title:** Vascular targeted radioimmunotherapy

## **ABSTRACT**

**Rationale:** Glioblastoma is characterized by an aggressive and aberrant vascular network that promotes tumor progression and hinders effective treatment; the median survival is 16 months despite standard-of-care therapies. There is a need to improve therapeutic options for this disease. We hypothesized that antibody targeting of the vascular endothelium (VE) of glioblastoma with cytotoxic short-range, high-energy alpha particles would be an effective therapeutic approach.

**Methods:** E4G10, an antibody directed at an epitope of monomeric VE cadherin, is expressed in tumor neovasculature and on endothelial progenitor cells in the bone marrow. E4G10 was labeled with alpha particle emitting  $^{225}\text{Actinium}$  ( $^{225}\text{Ac}$ ). Pharmacokinetic studies investigated the tissue distribution and blood clearance of the  $^{225}\text{Ac}$ -E4G10 radioimmunoconstruct in a transgenic Ntva-mouse model of high-grade glioblastoma. Histological analysis was used to demonstrate local therapeutic effects in treated brain tumor sections. Radioimmunotherapy with  $^{225}\text{Ac}$ -E4G10 was performed in Ntva-mice to assess overall survival alone and in combination with temozolomide, the standard-of-care chemotherapeutic agent.

**Results:**  $^{225}\text{Ac}$ -E4G10 was found to accumulate in tissues expressing the target antigen. Anti-vascular alpha-particle therapy of glioblastoma in the transgenic Ntva-model resulted in significantly improved survival compared to controls and potent control of tumor growth. Adding the chemotherapeutic temozolomide to the treatment increased survival to 30 days (versus 9 days for vehicle treated animals). Histological analyses showed a remodeled glioblastoma vascular microenvironment.

**Conclusion:** Targeted alpha-particle anti-vascular therapy is shown for the first time to be effective in increasing overall survival in a solid tumor in a clinically relevant transgenic glioblastoma mouse model.

## INTRODUCTION

Glioblastoma is a malignant astrocytoma and one of the most rapidly fatal and incurable cancers (1). These aggressive tumors are highly invasive and their cellular processes can often extend several centimeters away from the primary lesion. Standard intervention is surgical resection followed by field radiotherapy (total dose of up to 60 Gy). Chemotherapy improves the outcome, but, despite the aggressive combination of surgery, radiotherapy and chemotherapy, the median survival is only sixteen months (2). Clinical outcomes for patients with glioblastoma have remained the same for many years despite numerous attempts to improve the standard-of-care. The probability of two-year survival is less than 30% with optimal therapy (3). There is a need to provide better therapeutic options for this disease.

Glioblastoma is among the most vascularized tumors (4), making it an ideal target for anti-vascular therapies (5). Bevacizumab, the first clinically validated anti-angiogenic therapeutic for glioblastoma, inhibits vascular endothelial growth factor A-signaling, which has a central role in blood vessel growth (6). However, systemic toxicity has been an important issue when treating with bevacizumab (7), as well as observed resistance to the treatment (8) and only minimally improved survival benefit.

Damaging the tumors vascular endothelium (VE) is another anti-vascular therapeutic strategy (9,10). Alpha particles are emitted charged helium nuclei that travel only several cell diameters (40-80  $\mu\text{m}$ ). Individual alpha particles deposit 5-8 MeV of energy over a short, densely ionizing track, causing cell death. This is ten to one hundred times more energy than is released in a beta particle emission typically used in radioimmunotherapy. Alpha particles are lethal when emitted in the vicinity of a target cell, but spare normal bystander tissue outside its short range (11-13). This characteristic particle energy and geometry offers clear advantages over other known forms of radiation as a means of precision cell killing, particularly in the brain.  $^{225}\text{Actinium}$  is an alpha particle emitting radionuclide with a 10.0 d half-life; that along with its daughters release 4 alpha particle emissions, each individually lethal to cells in their path. This  $^{225}\text{Ac}$ -antibody drug strategy has been described as an atomic nanogenerator for in vivo delivery of alpha particles to tumor (12).

Alpha particle emitting radionuclides are among the most potent cytotoxic agents known and the approval of Xofigo ( $^{223}\text{Ra}$  chloride) by the Food and Drug Administration demonstrated the effectiveness and safety of targeted alpha particle therapy (14). We translated  $^{225}\text{Ac}$ -lintuzumab

into clinical trials against leukemia (15). To date, we have completed a crucial Phase I study of  $^{225}\text{Ac}$ -lintuzumab demonstrating safety and biological activity, leading to a multi-center Phase I/II trial to determine the maximum tolerated dose, toxicity and efficacy of fractionated-doses of  $^{225}\text{Ac}$ -lintuzumab in combination with low-dose cytarabine. We brought this knowledge to bear on the development of the VE-targeted antibody, E4G10, a monoclonal antibody that binds to an epitope of monomeric VE-cadherin, that is expressed by angiogenic VE (16,17) and bone marrow-derived endothelial progenitor cells (18). Importantly, E4G10 binds to an epitope present only on monomeric VE-cadherin but not the homodimeric form found in established resting vasculature, thus conferring specificity for tumor vessels and endothelial progenitor cells.

Here we report the first preclinical investigation of cytotoxic alpha particle irradiation as anti-vascular treatment of high grade glioblastoma in a transgenic mouse model of rapidly progressing disease. We first investigate the biodistribution of the  $^{225}\text{Ac}$ -E4G10 radioimmunoconstruct in naïve and glioblastoma bearing mice and show local histological response to the treatment in brain tumor tissue. In survival studies we explore the therapeutic ability of radioimmunotherapy with  $^{225}\text{Ac}$ -E4G10 in Ntva-mice as standalone therapy and in combination with the standard-of-care chemotherapeutic temozolamide. Targeted alpha-particle anti-vascular therapy is investigated for the first time in a solid tumor in a relevant transgenic glioblastoma mouse model.

## MATERIALS AND METHODS

### Radiochemistry

$^{225}\text{Ac}$  (ORNL, Oak Ridge, TN) was conjugated to the anti-VE-cadherin IgG2a rat antibody, E4G10 (Eli Lilly and Company, New York, NY) or an isotype-matched control antibody (IgG2a, anti-Keyhole Limpet Haemocyanin, R&D Systems, Minneapolis, MN) and purified and analyzed for radiolabeling quality as described previously (19,20). The purified radioimmunoconstructs were formulated in 1% human serum albumin (HSA, Swiss Red Cross, Bern, Switzerland) and 0.9% sodium chloride (Normal Saline Solution, Abbott Laboratories, North Chicago, IL) for intravenous injection.

### Glioblastoma animal model

The Nestin-tumor virus A (Ntva)-mouse (Ink4a-Arf<sup>-/-</sup>; FVB/N, C57BL6 and BALB/C background) with the retroviral RCAS (replication-competent avian sarcoma-leukosis virus) system was previously described (21) and used for all studies *in vivo*. The RCAS vector carries the tumor-driver human platelet-derived growth factor B and is overexpressed by chicken DF-1 cells. Tumor induction was performed at the age of four to ten weeks by stereotactic delivery of  $2 \times 10^5$  chicken DF-1 cells (1 µl) intracranially at 1 mm caudal and 1.5 mm lateral from bregma into the right frontal cortex (injection depth 2 mm) of Ntva-mice.

### **Experimental design for studies *in vivo***

Tumor growth and progression of glioblastoma induced Ntva-mice was assessed by performing T2 Magnetic Resonance Imaging (MRI) five weeks after induction. Animals were subsequently placed into treatment groups with a distribution of tumor sizes and treated with either 0.1 ml radioimmunoconstruct or injection vehicle, respectively, via retro-orbital venous plexus. Animals were monitored for survival or sacrificed ten days after the treatment and tissues harvested for analysis.

### **T2 MRI**

Mice were MR imaged to quantify initial tumor volumes for therapeutic studies and to assess treatment responses with a custom-made ID 32-mm quadrature birdcage body resonator (Stark Contrast MRI Research, Erlangen, Germany) while anesthetized under 1.5% isoflurane. All images were acquired on a Bruker USR 4.7T scanner (Bruker Biospin MRI Inc., Billerica, MA). The mouse head was imaged in coronal orientation using a T2-weighted fast spin-echo RARE sequence (TR=3.5 s, TE=50 ms, RARE factor of 8, NEX=24, FOV=3×2 cm, slice thickness = 0.7 mm or 1 mm, in-plane resolution of 117×156 µm).

### **Pharmacokinetic profile of radioimmunoconstructs**

Twenty-four Ntva-mice with glioblastoma were MR imaged for tumor growth and tumor sizes and placed in eight groups (n=3); 40 naïve Ntva-mice were arranged into eight groups (n=5). Each animal received a single intravenous dose of 11.1 kBq (300 nCi) of  $^{225}\text{Ac}$ -E4G10 or  $^{225}\text{Ac}$ -isotype. Mice were euthanized at 4, 12, 36 and 240h and tissue samples were harvested, weighed and counted in a  $\gamma$ -counter using a 360-480 KeV window at secular equilibrium. Aliquots (20 µl)

of the injected doses were used as decay correction standards. The percentage of injected dose per gram of tissue weight (%ID/g) were calculated and plotted as means. Statistical analysis of data was performed using Prism software (Graphpad Software Inc, La Jolla, CA).

### **Absorbed dose estimates**

%ID/g values were converted to percentage of injected activity per gram of tissue weight (%IA/g). Thereafter, the areas under the activity concentration-time curves were estimated by trapezoidal integration with the contribution of the terminal portion calculated by extrapolation from the 240h value using the faster of apparent terminal clearance rate or physical decay. Subsequently, absorbed doses, D (Gy/MBq), were calculated from the area under the curve (%IA h/g) values according to  $D = 10 \times \text{area under the curve} \times \Delta$ , where  $\Delta$  is the equilibrium dose constant for the total decay of  $^{225}\text{Ac}$ . The value used for  $\Delta$  ( $1.43 \times 10^{-2}$  J/MBq h) includes the contributions of all the radioactive progeny of  $^{225}\text{Ac}$  and thus assumes no translocation of any progeny from the site of the original  $^{225}\text{Ac}$  decay.

### **Histological analysis**

Glioblastoma-bearing Ntva-mice (n=12) were placed into the following groups with an even distribution of tumor sizes:  $^{225}\text{Ac}$ -E4G10 (n=4),  $^{225}\text{Ac}$ -isotype (n=4) and 1% HSA vehicle (n=4). Anesthetized (1.5% isoflurane) mice received a single 7.4 kBq (200 nCi) dose (0.1 ml) via retro-orbital venous plexus of  $^{225}\text{Ac}$ -E4G10,  $^{225}\text{Ac}$ -isotype control or vehicle at day 0. Ten days after treatment tumor was harvested and analyzed. Briefly, mice were sacrificed and glioblastoma and brain were excised and fixed in 4% paraformaldehyde/phosphate-buffered saline for 2 days. Fixed tissue was paraffin-embedded and cut into 5  $\mu\text{m}$  sections. Sections were stained with hematoxylin-eosin or anti-CD31 antibody for endothelium, respectively. Sections were scanned with the Mirax Digital Slide Scanner using a 20 $\times$  lens (Carl Zeiss Microimaging, Jena, Germany). Analysis was performed on whole tumor sections with Pannoramic Viewer software (3DHISTECH, Budapest, Hungary).

### **Survival studies**

Therapy was conducted for all survival studies following the initial MR imaging 5 weeks after induction. Tumor induction with the RCAS system resulted in a normal distribution of tumor

sizes and disease progression in tumor-induced mice (60-80% of tumors small/medium sized; 10-20% very small/not visible in the initial MRI; 10-20% were large tumors occupying up to 20% of cranial space). Mice with large tumor sizes exhibited glioblastoma symptoms like hydrocephalus or hunched posture and were excluded from entering studies (as well as animals exhibiting very small/not-yet visible tumors). However, these late stage animals entered survival study II to investigate therapy results in a late-stage disease scenario. Survival outcomes were scored and plotted using Kaplan-Meier survival analysis in prism software.

### **Survival study I**

Mice were separated into a  $^{225}\text{Ac}$ -E4G10 treatment group (n=9) and a 1% HSA (vehicle) group (n=8) and treated with 0.46 kBq (12.5 nCi)  $^{225}\text{Ac}$ -E4G10/g body mass (7.4-11.1 kBq (200-300 nCi)/mouse). Tumor growth was followed in four representative mice per group using T2 MRI to measure tumor volume at baseline (day 0; 5 weeks after tumor induction) and 10 days later.

### **Survival study II**

Mice treated in survival study II exhibited advanced glioblastoma with symptoms of hydrocephalus and hunched posture. Mice were separated into a specific  $^{225}\text{Ac}$ -E4G10 treatment group (n=4), a control  $^{225}\text{Ac}$ -isotype group (n=3), and a 1% HSA vehicle-only control group (n=6). Mice were treated 5 weeks post-tumor induction with 0.46 kBq (12.5 nCi)/g body mass (7.4-11.1 kBq (200-300 nCi)/mouse) or with the 1% HSA injection vehicle.

### **Survival study III**

Animals in the  $^{225}\text{Ac}$ -E4G10 + temozolomide group (n=10) received 0.46 kBq (12.5 nCi)/g body mass (7.4-11.1 kBq (200-300 nCi)/mouse)  $^{225}\text{Ac}$ -E4G10 and a cumulative dose of 10 mg temozolomide (5×2 mg) via oral gavage using a 12% dimethyl sulfoxide/normal saline solution vehicle on days 0-4. Animals in the temozolomide group received a cumulative dose of 10 mg of temozolomide (5×2 mg) via oral gavage using a 12% dimethyl sulfoxide/normal saline solution vehicle on days 0-4.

### **Statistical analysis**

Statistical analysis of data was performed using Prism software (Graphpad Software Inc, La Jolla, CA). Data are displayed as means with their standard errors (SEM). P-values for comparisons between treatment groups were obtained in GraphPad Prism using Student's t-test for statistical significance (unpaired, two-tailed t-test). *P*-values < 0.05 were considered statistically significant. Log-rank (Mantel-Cox) and Mantel-Haenszel tests were used to compare survival outcomes.

## **Study approval**

All animal experiments were done in accordance with the NIH guide for the care and use of laboratory animals and approved by the Institutional Animal Care and Use Committee of Memorial Sloan Kettering Cancer Institute.

## **RESULTS**

### **The radioimmunotherapeutic drug $^{225}\text{Ac}$ -E4G10 and the Ntva-animal model**

The transgenic Ntva-mouse modeled the Platelet-derived growth factor-driven proneural glioblastoma subtype of human disease and was used to evaluate  $^{225}\text{Ac}$ -E4G10 in therapeutic studies (21). Radiolabeling results were similar for the specific antibody E4G10 and the isotype control antibody used in therapeutic and mechanistic studies. The  $^{225}\text{Ac}$ -E4G10 constructs were  $97.6\% \pm 2.4\%$  radiochemically pure (mean  $\pm$  standard deviation, (*n*=16)) and had specific activities of  $7.03 \pm 3.70$  GBq ( $0.19 \pm 0.10$  Ci)/g. The  $^{225}\text{Ac}$ -isotype was  $98.7\% \pm 0.84\%$  (*n*=10) radiochemically pure and had specific activities of  $4.81 \pm 2.96$  GBq ( $0.13 \pm 0.08$  Ci)/g.

### **Pharmacokinetic profile of $^{225}\text{Ac}$ -E4G10 in naïve and glioblastoma Ntva-mice**

The biodistribution of  $^{225}\text{Ac}$ -E4G10 and  $^{225}\text{Ac}$ -isotype was profiled in Ntva-mice with and without glioblastoma as a function of time (Fig. 1; Supplementary Fig. 1).  $^{225}\text{Ac}$ -E4G10 cleared from the blood in glioblastoma mice within the first 2d of treatment (Figs. 1A and 2A) while naïve Ntva-mice cleared the drug more slowly from the blood (Fig. 2B), presumably because in the mice with tumor there were sinks for the drug to accumulate. The low activity accumulated in tumor can be attributed to the small number of monomeric VE-cadherin<sup>+</sup>-cells being targeted in the mouse (n.b. the tumor cells are not targeted directly with this drug). Plotting the activity

measured in the tumor and bone (which includes the red marrow) normalized to blood activity (Figs. 2C and 2D) reveals a time-dependent enrichment of the labeled antibody in glioblastoma/brain and bone versus blood. Monomeric VE-cadherin is expressed both in the glioblastoma vasculature and the endothelial progenitor cells in the red marrow. The glioblastoma and bone data normalized to blood activity shows less accumulation of the isotype control drug construct. The  $^{225}\text{Ac}$ -isotype control antibody exhibited a prolonged blood half-life compared to  $^{225}\text{Ac}$ -E4G10 (Supplementary Fig. 1; Fig. 2A); 11.5% in the blood at 36h and 5.2% at 240h (versus 1.8% at 36h in the  $^{225}\text{Ac}$ -E4G10 group).

### Absorbed dose estimates of $^{225}\text{Ac}$ -E4G10 in naïve and glioblastoma Ntva-mice

We performed dosimetry calculations from the biodistribution data to estimate the tumor absorbed dose and to estimate doses to non-targeted tissues (Supplementary Table 1). The estimated absorbed dose of  $^{225}\text{Ac}$ -E4G10 in glioblastoma bearing mice for tumor/brain was found to be  $24.4 \pm 4.8$  Gy/MBq. In comparison, the estimated dose to healthy brain was  $3.1 \pm 0.8$  Gy/MBq. Hence, the estimated absorbed dose to tumor tissue was 7.7 times higher than that to healthy brain tissue ( $P = 0.016$ ).

### Histological response to $^{225}\text{Ac}$ -E4G10 treatment

The gross architecture of the glioblastoma vascular endothelial microenvironment changed as a result of  $^{225}\text{Ac}$ -E4G10 therapy. Glioblastoma tissue sections were examined 10d post-therapy with hematoxylin-eosin staining and anti-CD31 endothelial cell marker (Fig. 3). Vehicle treated tumors showed characteristic hematoxylin-eosin morphology for high grade glioblastoma. Massive branches of vasculature are visible and the cellularity is increased. The tumor vasculature is morphologically distinct from healthy brain. Vessels in glioblastoma spread without organization, are tortuous and show massive extensions in all directions. They are leaky (edematous), dilated, irregular in shape and with diameters up to 100  $\mu\text{m}$ . A single dose of  $^{225}\text{Ac}$ -E4G10 leads to significant glioblastoma VE remodeling. These mice exhibited structural vascular changes with features analogous to healthy brain where vessels are significantly smaller in size and diameter compared to controls. There are more necrotic regions noted in the vehicle and isotype control antibody groups as well as a greater CD31 density ( $P = 0.038$ ) compared to vehicle treated controls (Fig. 3B). The intermediate changes in CD31 arising from  $^{225}\text{Ac}$ -isotype

were attributed to nonspecific irradiation from the activity that persisted in blood (Fig. 2C; Figs. 3A and 3B).

### **Vascular targeting $^{225}\text{Ac}$ -E4G10 controls tumor growth**

Tumors in animals treated with  $^{225}\text{Ac}$ -E4G10 in survival study I were significantly smaller compared to tumors in the vehicle treated group ( $P = 0.017$ , Figs. 4A and 4B) 10 days post therapy. T2 MRI of four representative animals per group of animals from survival study I showed that baseline tumor volumes at day 0 of treatment (5 weeks after induction) were  $31.5 \pm 13.0 \text{ mm}^3$  and  $10.0 \pm 4.9 \text{ mm}^3$  in the vehicle and E4G10 groups, respectively. On day 10, animals in the vehicle treated group had mean tumor volumes of  $171.7 \pm 28.6 \text{ mm}^3$  versus  $42.7 \pm 26.9 \text{ mm}^3$  for  $^{225}\text{Ac}$ -E4G10 treated animals. At the start of therapy approximately 4% (on average) of the cranial space was occupied by glioblastoma and by day 10, the untreated control mice had tumor volumes occupying approximately 35% on average of the cranial space.

### **$^{225}\text{Ac}$ -E4G10 radioimmunotherapy of the glioblastoma vasculature significantly increases survival**

In survival study I (Fig. 5A) we asked whether  $^{225}\text{Ac}$ -E4G10 treatment improves overall survival of glioblastoma bearing Ntva-mice and whether the radioimmunoconstruct was active towards inhibiting glioblastoma growth (Fig. 4B). Treatment with  $^{225}\text{Ac}$ -E4G10 was found to significantly prolong median survival compared to controls. The median survival in the  $^{225}\text{Ac}$ -E4G10 group was 21d compared to 9d in the vehicle group ( $P = 0.0002$ , Fig. 5A). Survival study II was conducted to demonstrate efficacy of treatment in animals with advanced disease symptoms and to show specificity of  $^{225}\text{Ac}$ -E4G10 for increasing survival by comparison to the  $^{225}\text{Ac}$ -labelled isotype control antibody or vehicle (Fig. 5B).  $^{225}\text{Ac}$ -E4G10 treatment prolonged median survival significantly compared to controls. The three groups had median survival values of 11d for  $^{225}\text{Ac}$ -E4G10 versus 7d for  $^{225}\text{Ac}$ -isotype versus 5d for the vehicle group, respectively. Survival study III (Fig. 5C) compared the efficacy of combined  $^{225}\text{Ac}$ -E4G10 radioimmunotherapy and temozolomide chemotherapy in groups of mice with glioblastoma. The combinational therapy prolonged the median survival of Ntva-mice to 30d in the  $^{225}\text{Ac}$ -E4G10+ temozolomide group versus 26d in the temozolomide-only group. The survival benefit in the

combination group was not statistically different than temozolomide alone ( $P = 0.128$ ). However, the Kaplan-Mayer plot of study III shows an extended survival tail, reflecting the  $^{225}\text{Ac-E4G10+}$  temozolomide therapeutic benefit. 40% of animals in the combination therapy group are still alive on day 32 compared to 0% in the temozolomide-only group. The hazard ratio was found to be 0.4973 ( $^{225}\text{Ac-E4G10+temozolomide}/\text{temozolomide}$ ), expressing the survival benefit for animals in the combined therapy group.

## DISCUSSION

Glioblastoma is one of the most aggressive and vascularized tumors and therefore a strategic objective for the potent anti-vascular  $^{225}\text{Ac-E4G10}$  drug. We have reported the therapeutic effectiveness of  $^{225}\text{Ac-E4G10}$  directed against xenografted carcinoma VE and bone marrow-endothelial progenitor cells (18,22-24) and now directed this drug against the VE of glioblastoma. We wanted to explore the therapeutic potential of  $^{225}\text{Ac-E4G10}$  arising from changes produced by alpha irradiation in the glioblastoma vasculature. The glioblastoma blood brain barrier presents a unique vascular microenvironment compared to the other carcinoma models that we have studied. The Ntva-model is a genetically engineered mouse that recapitulates the genetics and histology of the human glioblastoma (21,25) and provided a relevant orthotopic model for our investigations. Moreover, Ntva-mice are not immunodeficient, which permits the interpretation of therapy outcomes under immunocompetent background.

Alpha particles have been proven to be potent therapeutic effectors when directed at cancer targets (11,12). The short effective range (several cell diameters) and high energies (5-8 MeV) of these particles make them ideal for targeting the aggressive growing tumor vasculature of glioblastoma while imparting minimal bystander radiation damage to the healthy brain tissue. The therapeutic efficacy of  $^{225}\text{Ac-E4G10}$  was significant, improving survival versus vehicle treated controls;  $^{225}\text{Ac-E4G10}$  increased survival from 9 days to 21 days. MRI measurements comparing the tumor volumes of vehicle-treated versus  $^{225}\text{Ac-E4G10}$  showed potent tumor growth control. Treatment efficacy and specificity of  $^{225}\text{Ac-E4G10}$  was demonstrated in animals with advanced disease (hydrocephalus and hunched posture) in a survival study versus  $^{225}\text{Ac}$ -isotype and vehicle controls. The combination of  $^{225}\text{Ac-E4G10}$  and temozolomide increased median survival of glioblastoma mice further to 30d versus 21d. There was no significant survival difference for the combination therapy compared to temozolomide-only; however, we

did observe a long-tailed survival curve, indicating a survival benefit in mice treated with radioimmunotherapy plus chemotherapy. Moreover, the hazard ratio showed a survival benefit in the combination group. Temozolomide is currently the chemotherapeutic of choice for the treatment of human glioblastoma; it is a cytotoxic prodrug that methylates nucleotide bases and inhibits DNA replication following hydrolysis (26). Improving temozolomide delivery to glioblastoma as a result of vascular remodeling would be an advantage in this drug's use.

$^{225}\text{Ac}$ -E4G10 treated animals in survival studies eventually progressed and succumbed to the disease. However, we conducted our alpha-particle therapy studies with a single dose of  $^{225}\text{Ac}$ -E4G10 to provide therapeutic proof-of-concept and to demonstrate feasibility and efficacy of anti-vascular therapy with  $^{225}\text{Ac}$ -E4G10 in glioblastoma mice. Multiple  $^{225}\text{Ac}$ -E4G10 treatments and optimization of drug scheduling of combined therapies could be used to maximize therapeutic effect.

The pharmacokinetic distribution of  $^{225}\text{Ac}$ -E4G10 in the Ntva-mouse model showed drug accumulation in tumor and bone marrow versus the isotype control ten days after administration. Both tissues express monomeric VE-cadherin and are therefore sinks for  $^{225}\text{Ac}$ -E4G10 accumulation. The correlative data from naïve animals supports this result. We found moreover a 7.7-fold increase in absorbed dose of  $^{225}\text{Ac}$ -E4G10 to glioblastoma versus healthy brain tissue in naïve mice, explaining efficacy of the radioimmunoconstruct in tumor tissue. Histological analysis of  $^{225}\text{Ac}$ -E4G10 treated glioblastoma brain tissue showed an overall vascular depletion and a remodeled microenvironment. We observed a 64% drop in overall vascularity; vessels were smaller in size and better distributed over the whole tissue.

Estimates of absorbed doses to healthy tissues are crucial for toxicity estimates when treating with alpha particles (27). We found >20% ID/g of  $^{225}\text{Ac}$ -E4G10 in the liver ten days after treatment and the estimated dose to liver was the highest among non-targeted tissues (1577 Gy/MBq in glioblastoma animals). However, similar or even higher doses to liver have been observed with the alpha emitter  $^{213}\text{Bi}$  in leukemia patients treated with  $^{213}\text{Bi}$ -lintuzumab (28), and no liver toxicity was noted in this study or the  $^{225}\text{Ac}$ -lintuzumab clinical trials (29).

The concurrent processes of vasculogenesis, angiogenesis and tumor proliferation are keys to tumor growth and dissemination and interrelated by a paracrine effect. Disrupting and damaging the vascular endothelial architecture associated with tumor tissue is a recognized therapeutic strategy. This approach has been used clinically, with the approval of several anti-angiogenic

agents by the Food and Drug Administration. However, systemic toxicity and therapy resistance have been an important issue when treating with bevacizumab and other anti-angiogenic agents. Importantly, our drug acts primarily through direct cell killing, rather than through action on signaling networks and without the global side-effects on the angiogenesis axis that other anti-angiogenic drugs may promote. Furthermore, targeting endothelial cells in the inner lumen of the glioblastoma vasculature with this macromolecular radioimmunotherapeutic agent permits systemic administration and importantly, does not require transit across the blood brain barrier and penetration into the tumor. The requirement to cross the blood brain barrier and accumulate in tumor could be a major hurdle for other glioblastoma targeting agents.

## CONCLUSION

In conclusion, our preclinical studies in the Ntva- mouse model found promising potential of <sup>225</sup>Ac-E4G10 therapy as anti-vascular treatment for glioblastoma. We demonstrated in survival studies that radioimmunotherapy with <sup>225</sup>Ac-E4G10 in Ntva-mice increased overall survival as standalone therapy from 9 to 21 days and controlled tumor growth. Survival was further increased to 30 days if the treatment was applied in combination with the standard-of-care chemotherapeutic temozolomide. We showed for the first time how an alpha targeting anti-vascular drug in a relevant transgenic mouse model of glioblastoma improved survival. In view of future clinical development of <sup>225</sup>Ac-E4G10 as anti-vascular treatment for the therapy of glioblastoma, further studies investigating the mechanism of action of <sup>225</sup>Ac-E4G10 in the Ntva-mouse model are necessary. We are currently investigating the changes in the architecture of the vasculature and tumor microenvironment caused by alpha particle radiation in Ntva-mice. Mechanistic studies will inform on the observed survival benefit upon radioimmunotherapy reported herein using the <sup>225</sup>Ac-E4G10 drug in the glioblastoma Ntva-mouse model.

## ACKNOWLEDGMENTS

This work was supported by the NIH R01 CA166078, R01 CA55349, R25T CA046945, R24 CA83084, P30 CA08748, P01 CA33049, F31 CA167863, the MSK Experimental Brain Tumor Center, Mr. William H. and Mrs. Alice Goodwin and the Commonwealth Foundation for Cancer Research, The MSK Center for Experimental Therapeutics and the MSK Center for Molecular Imaging and Nanotechnology. We thank Eli Lilly and Company for the E4G10 antibody,

Pharmactinium, Inc., for  $^{225}\text{Ac}$ , Dr. Eric Holland and Dr. Johanna Joyce for breeding pairs and the MSKCC Molecular Cytology Core Facility.

## REFERENCES

- (1) Dunn GP, Rinne ML, Wykosky J, et al. Emerging insights into the molecular and cellular basis of glioblastoma. *Genes Dev.* 2012;26:756-784.
- (2) Chinot OL, Wick W, Mason W, et al. Bevacizumab plus radiotherapy-temozolomide for newly diagnosed glioblastoma. *N Engl J Med.* 2014;370:709-722.
- (3) Norden AD, Wen PY. Glioma therapy in adults. *Neurologist.* 2006;12:279-292.
- (4) Tuettenberg J, Friedel C, Vajkoczy P. Angiogenesis in malignant glioma-a target for antitumor therapy? *Crit Rev Oncol Hematol.* 2006;59:181-193.
- (5) Jain RK, di Tomaso E, Duda DG, Loeffler JS, Sorensen AG, Batchelor TT. Angiogenesis in brain tumours. *Nat Rev Neurosci.* 2007;8:610-622.
- (6) Cloughesy TF, Cavenee WK, Mischel PS. Glioblastoma: from molecular pathology to targeted treatment. *Annu Rev Pathol.* 2014;9:1-25.
- (7) Ranpura V, Hapani S, Wu S. Treatment-related mortality with bevacizumab in cancer patients: a meta-analysis. *JAMA.* 2011;305:487-494.
- (8) Bergers G, Hanahan D. Modes of resistance to anti-angiogenic therapy. *Nat Rev Cancer.* 2008;8:592-603.
- (9) Kerbel RS. Antiangiogenic therapy: a universal chemosensitization strategy for cancer? *Science.* 2006;312:1171-1175.
- (10) Jain RK. Normalization of tumor vasculature: an emerging concept in antiangiogenic therapy. *Science.* 2005;307:58-62.
- (11) McDevitt MR, Sgouros G, Finn RD, et al. Radioimmunotherapy with alpha-emitting nuclides. *Eur J Nucl Med.* 1998;25:1341-1351.
- (12) McDevitt MR, Ma D, Lai LT, et al. Tumor therapy with targeted atomic nanogenerators. *Science.* 2001;294:1537-1540.

- (13) Sgouros G, Hobbs RF, Song H. Modelling and dosimetry for alpha-particle therapy. *Curr Radiopharm.* 2011;4:261-265.
- (14) FDA approves radiopharmaceutical for metastatic prostate cancer (News report). *Cancer Discov.* 2013;3:OF1.
- (15) Sgouros G, Roeske JC, McDevitt MR, et al. MIRD pamphlet no. 22 (abridged): radiobiology and dosimetry of alpha-particle emitters for targeted radionuclide therapy. *J Nucl Med.* 2010;51:311-328.
- (16) Liao F, Doody JF, Overholser J, et al. Selective targeting of angiogenic tumor vasculature by vascular endothelial-cadherin antibody inhibits tumor growth without affecting vascular permeability. *Cancer Res.* 2002;62:2567-2575.
- (17) May C, Doody JF, Abdullah R, et al. Identification of a transiently exposed VE-cadherin epitope that allows for specific targeting of an antibody to the tumor neovasculature. *Blood.* 2005;105:4337-4344.
- (18) Nolan DJ, Ciarrocchi A, Mellick AS, et al. Bone marrow-derived endothelial progenitor cells are a major determinant of nascent tumor neovascularization. *Genes Dev.* 2007;21:1546-1558.
- (19) Maguire WF, McDevitt MR, Smith-Jones PM, Scheinberg DA. Efficient 1-step radiolabeling of monoclonal antibodies to high specific activity with  $^{225}\text{Ac}$  for alpha-particle radioimmunotherapy of cancer. *J Nucl Med.* 2014;55:1492-1498.
- (20) McDevitt MR, Ma D, Simon J, Frank RK, Scheinberg DA. Design and synthesis of  $^{225}\text{Ac}$  radioimmunopharmaceuticals. *Appl Radiat Isot.* 2002;57:841-847.
- (21) Hambardzumyan D, Amankulor NM, Helmy KY, Becher OJ, Holland EC. Modeling adult gliomas using RCAS/t-va technology. *Transl Oncol.* 2009;2:89-95.
- (22) Escoria FE, Henke E, McDevitt MR, et al. Selective killing of tumor neovasculature paradoxically improves chemotherapy delivery to tumors. *Cancer Res.* 2010;70:9277-9286.

- (23) Ruggiero A, Villa CH, Holland JP, et al. Imaging and treating tumor vasculature with targeted radiolabeled carbon nanotubes. *Int J Nanomedicine*. 2010;5:783-802.
- (24) Singh JJ, Henke E, Seshan SV, et al. Selective alpha-particle mediated depletion of tumor vasculature with vascular normalization. *PLoS One*. 2007;2:e267.
- (25) Huse JT, Holland EC. Genetically engineered mouse models of brain cancer and the promise of preclinical testing. *Brain Pathol*. 2009;19:132-143.
- (26) Weller M, Cloughesy T, Perry JR, Wick W. Standards of care for treatment of recurrent glioblastoma-are we there yet? *Neuro Oncol*. 2013;15:4-27.
- (27) Akabani G, McLendon RE, Bigner DD, Zalutsky MR. Vascular targeted endoradiotherapy of tumors using alpha-particle-emitting compounds: theoretical analysis. *Int J Radiat Oncol Biol Phys*. 2002;54:1259-1275.
- (28) Sgouros G, Ballangrud AM, Jurcic JG, et al. Pharmacokinetics and dosimetry of an alpha-particle emitter labeled antibody:  $^{213}\text{Bi}$ -HuM195 (anti-CD33) in patients with leukemia. *J Nucl Med*. 1999;40:1935-1946.
- (29) Sgouros, G. (Ed.). MIRD radiobiology and dosimetry for radiopharmaceutical therapy with alpha-particle emitters. Reston, VA: *Society of Nuclear Medicine and Molecular Imaging, Inc.*; 2015.

## FIGURES

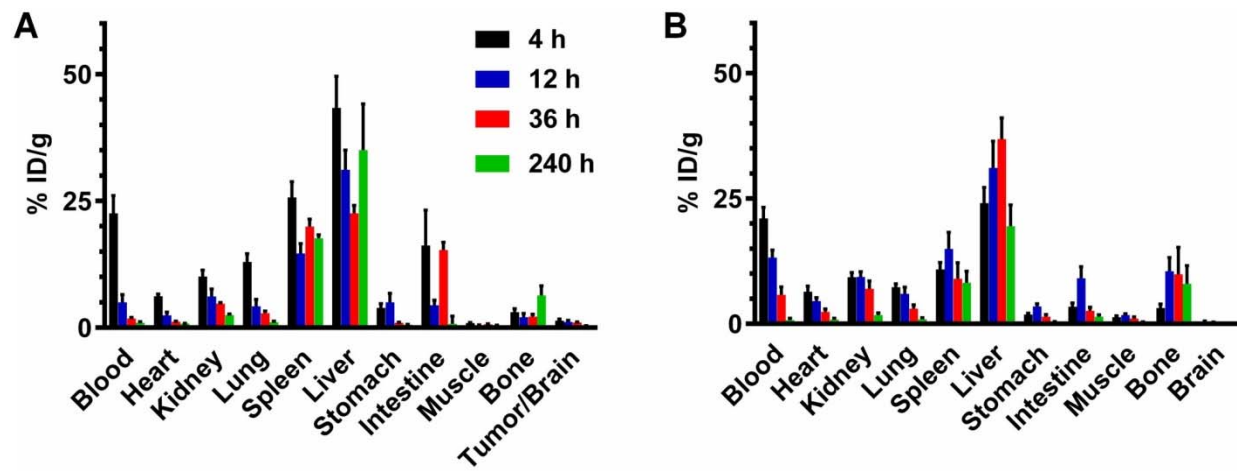


**FIGURE 1** Tissue biodistribution of A)  $^{225}\text{Ac}$ -E4G10 in glioblastoma tumor bearing mice and B)  $^{225}\text{Ac}$ -E4G10 in naïve mice. Shown is the tissue uptake in %ID/g at different time points. Reported values are means  $\pm$  SEM.

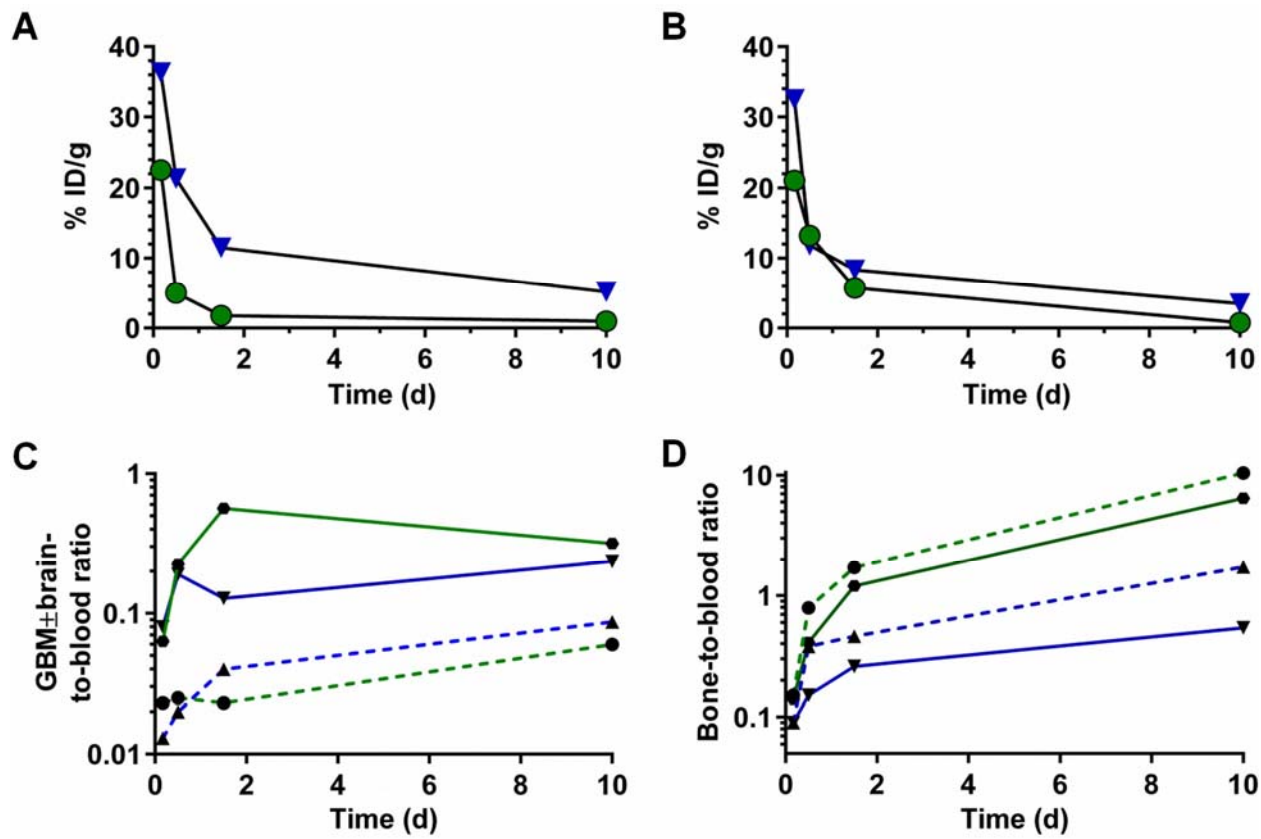


**FIGURE 2** Blood clearance of  $^{225}\text{Ac}$ -E4G10 and  $^{225}\text{Ac}$ -isotype control in A) glioblastoma bearing and B) naïve Ntva-mice. Green circles indicate  $^{225}\text{Ac}$ -E4G10 and blue triangles  $^{225}\text{Ac}$ -isotype. Reported values are % injected dose/g. C) Glioblastoma±brain-to-blood ratio and D) Bone-to-blood ratio illustrating the accumulation of  $^{225}\text{Ac}$ -E4G10 in the tumor and red bone marrow tissue. Relative ratios of glioblastoma±brain normalized to blood and bone normalized to blood are displayed. Green solid line is  $^{225}\text{Ac}$ -E4G10 in glioblastoma mice; green dashed line is  $^{225}\text{Ac}$ -E4G10 in naïve mice; blue solid line is  $^{225}\text{Ac}$ -isotype in glioblastoma mice; and blue dashed line is  $^{225}\text{Ac}$ -isotype in naïve mice.

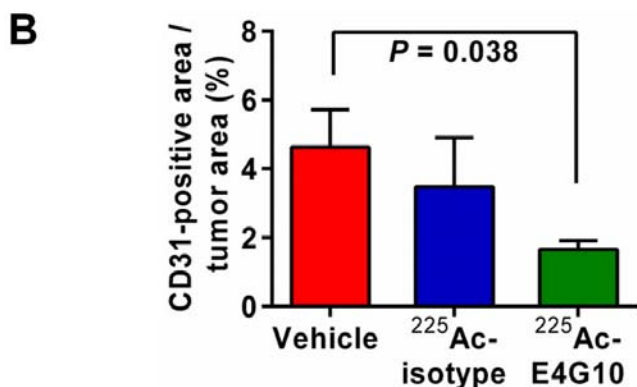
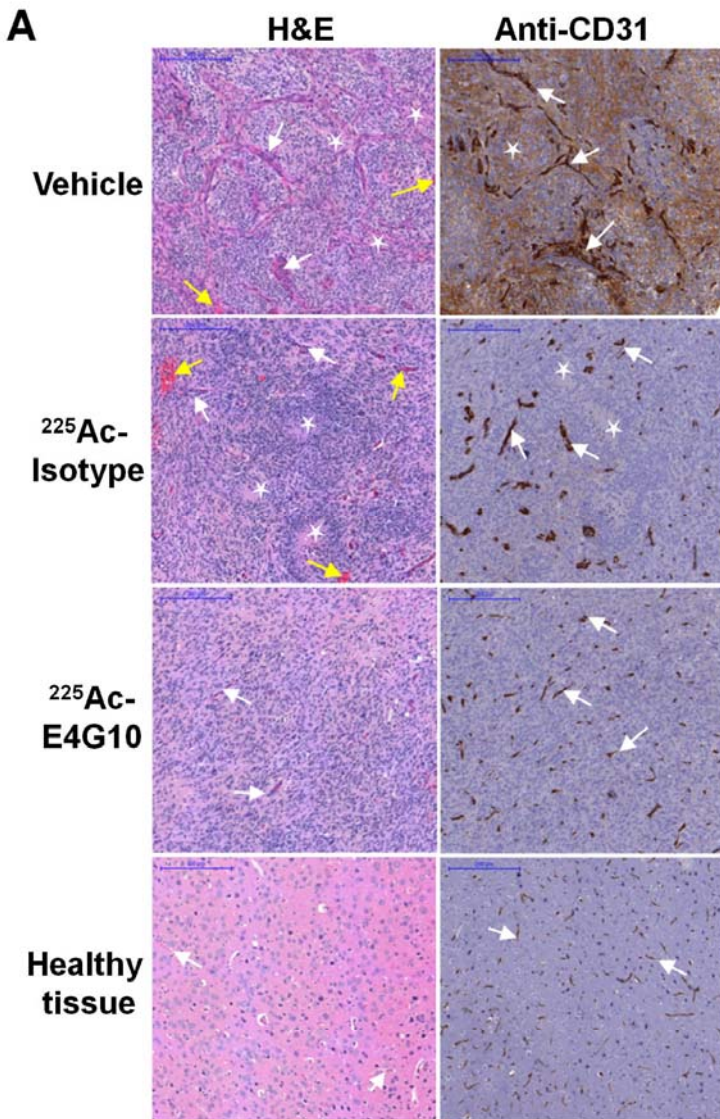


**FIGURE 3** Histological response of glioblastoma to targeted  $^{225}\text{Ac}$ -E4G10 therapy in Ntva-mice. A) Representative sections from treated glioblastoma Ntva-mice stained with hematoxylin-eosin (H&E) or anti-CD31 antibody for blood vessels. Healthy brain tissue is included for

comparison. Blood vessels are indicated by white arrows; necrosis is indicated with an asterisk; and hemorrhage is indicated with a yellow arrow. Scale bars are 200  $\mu\text{m}$  in all panels. B) Quantification of vascularity of whole anti-CD31 stained tumor sections of treated glioblastoma mice (n=4). Values are means  $\pm$  SEM.

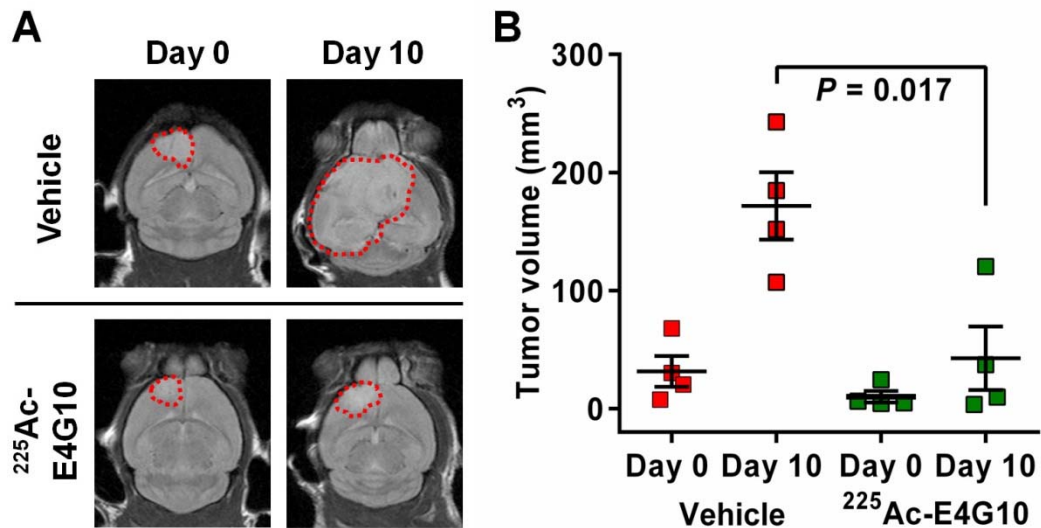


**FIGURE 4** Tumor sizes of glioblastoma bearing animals in survival study I before and 10 days after the treatment with either the specific treatment  $^{225}\text{Ac-E4G10}$  or the injection vehicle accessed by MRI. Shown is a T2 MR scan in coronal orientation of one representative animal of each group in A). Tumor margins are displayed as dashed red lines. B) Mean tumor volumes at day 0 and day 10 of vehicle treated (n=4) versus  $^{225}\text{Ac-E4G10}$  (n=4) treated animals. Reported values are means  $\pm$  SEM.

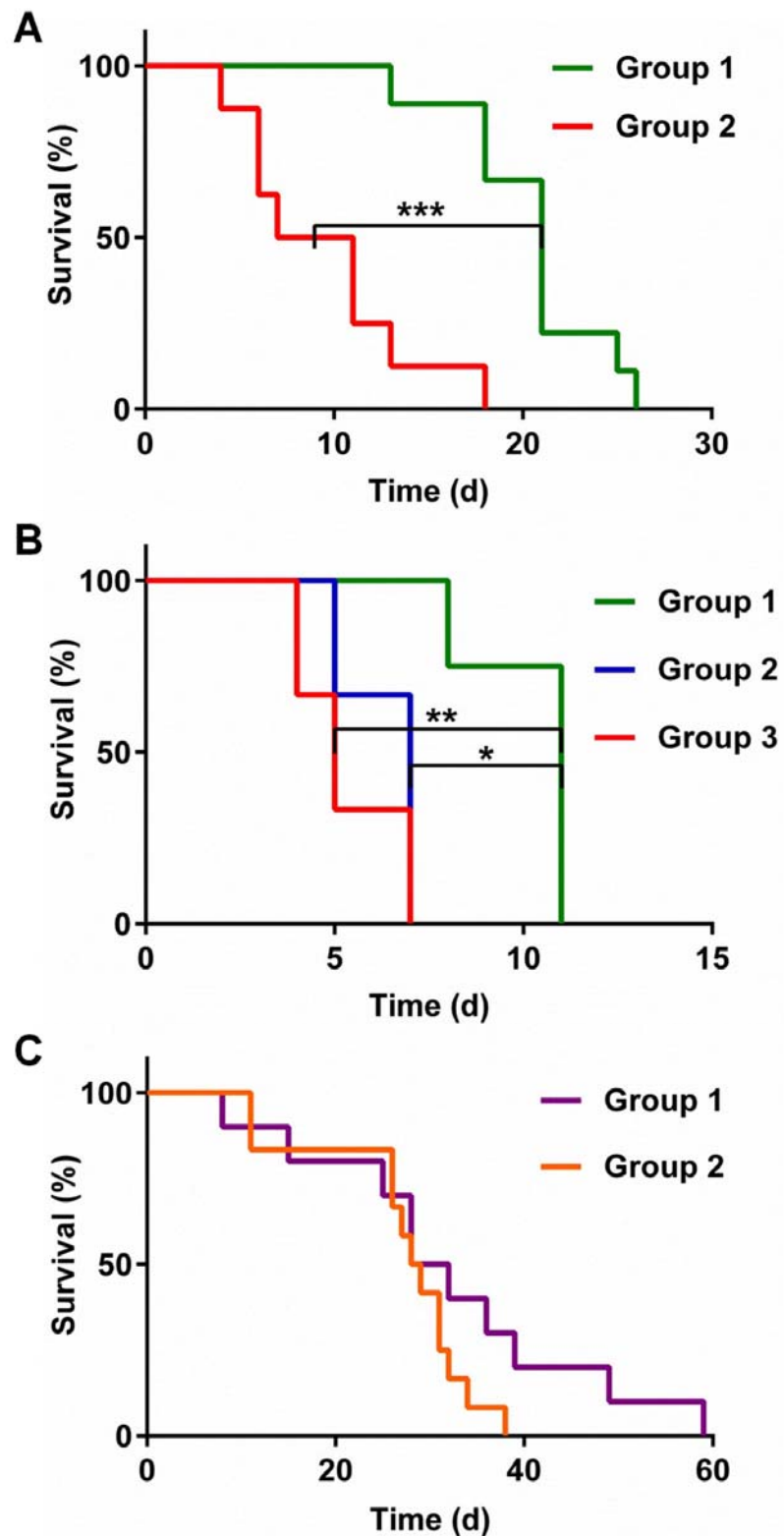


**FIGURE 5** Survival studies in Ntva-mice with glioblastoma. Kaplan-Meier survival curves of A) survival study I comparing the overall survival of  $^{225}\text{Ac}$ -E4G10 treated (Group 1) versus

vehicle treated (Group 2) Ntva-mice. \*\*\*  $P < 0.001$ . B) Survival study II showing overall survival after  $^{225}\text{Ac}$ -E4G10 (Group 1) therapy compared to unspecific therapy with  $^{225}\text{Ac}$ -isotype control antibody (Group 2) and vehicle treated controls (Group 3). Animals in survival study II exhibited advanced symptoms of disease. \*  $P < 0.05$ , \*\*  $P < 0.01$ . C) Survival study III comparing the overall survival of mice treated with combinational therapy with  $^{225}\text{Ac}$ -E4G10 radioimmunotherapy and temozolomide chemotherapy (Group 1) versus temozolomide-only (Group 2).